Morphological Characteristics of the Optic Nerve Head and Choroidal Thickness in High Myopia

Guangyi Hu,[1–6] Qiuying Chen,[1–6] Xian Xu,[1–6] Hanyi Lv,[1–6] Yuchen Du,[7] Lisheng Wang,[7] Yao Yin,[1–6] Ying Fan,[1–6] Haidong Zou,[1–6] Jiangnan He,[1–6] Jianfeng Zhu,[1–6] and Xun Xu[1–6]

[1]Department of Preventative Ophthalmology, Shanghai Eye Diseases Prevention and Treatment Center, Shanghai Eye Hospital, Shanghai, China
[2]Department of Ophthalmology, Shanghai General Hospital, Shanghai Jiao Tong University School of Medicine, Shanghai, China
[3]National Clinical Research Center for Eye Diseases, Shanghai, China
[4]Shanghai Key Laboratory of Ocular Fundus Diseases, Shanghai, China
[5]Shanghai Engineering Center for Visual Science and Photomedicine, Shanghai, China
[6]Shanghai Engineering Center for Precise Diagnosis and Treatment of Eye Diseases, Shanghai, China
[7]Department of Automation, Institute of Image Processing and Pattern Recognition, Shanghai Jiao Tong University, Shanghai, China

Correspondence: Jiangnan He, Department of Preventative Ophthalmology, Shanghai Eye Disease Prevention and Treatment Center, Shanghai Eye Hospital, No. 380 Kangding Road, Shanghai 200040, China; hejiangnan85@126.com.
Jianfeng Zhu, Department of Preventative Ophthalmology, Shanghai Eye Disease Prevention and Treatment Center, Shanghai Eye Hospital, No. 380 Kangding Road, Shanghai 200040, China; jfzhu1974@hotmail.com.
Xun Xu, Department of Preventative Ophthalmology, Shanghai Eye Disease Prevention and Treatment Center, Shanghai Eye Hospital, No. 380 Kangding Road, Shanghai 200040, China; drxuxun@sjtu.edu.cn.

GH and QC contributed equally to the work presented here and should therefore be regarded as equivalent authors.

Received: November 28, 2019
Accepted: March 10, 2020
Published: April 28, 2020

Citation: Hu G, Chen Q, Xu X, et al. Morphological characteristics of the optic nerve head and choroidal thickness in high myopia. *Invest Ophthalmol Vis Sci.* 2020;61(4):46. https://doi.org/10.1167/iovs.61.4.46

Purpose. This study aimed to explore the morphological characteristics of Bruch's membrane opening distance (BMOD), border length (BL), border tissue angle (BTA), vertical tilt angle, and peripapillary atrophy (PPA), as well as their associations with choroidal thickness (ChT) in young healthy highly myopic eyes.

Methods. A total of 167 patients with high myopia and 172 individuals without high myopia were enrolled. All of the subjects were divided by axial length. The PPA area was measured on fundus photographs. BMOD, BL, BTA, vertical tilt angle, macular ChT (mChT), and peripapillary ChT (pChT) were measured on swept-source optical coherence tomography scans.

Results. The PPA area ($P < 0.0001$) and vertical tilt angle ($P < 0.0001$) were larger, BMOD ($P < 0.0001$) and BL ($P < 0.0001$) were longer, and BTA ($P < 0.0001$) was smaller in the high-myopia group compared with the group without high myopia. Every 1-µm increase in BMOD was associated with a 35.80-µm decrease in mChT; every 1° decrease in BTA was correlated with a 0.32-µm decrease in mChT and a 0.26-µm decrease in pChT; and no association was found between PPA area and ChT in the multivariate linear regression model.

Conclusions. PPA area, BL, BMOD, and vertical tilt angle increased, but BTA decreased with axial elongation of the globe in young, healthy patients with myopia. Longer BMOD was positively correlated with lower mChT, and smaller BTA was positively correlated with lower mChT and pChT in this population.

Keywords: Bruch's membrane opening distance, border tissue angle, choroidal thickness, PPA area, young patients with myopia

High myopia is a major cause of visual impairment worldwide, especially in East Asian populations.[1,2] A higher prevalence of myopic maculopathy and high-myopia-associated glaucomatous optic neuropathy is associated with an increased degree of high myopia. Myopic maculopathy, a sight-threatening disorder, is the second most common reason for irreversible blindness in China.[3] Myopia has also been reported as an independent risk factor for glaucoma.[4–6] Furthermore, the morbidity rate of glaucoma increases along with an increase in the degree of myopia.[5] Optic nerve

head (ONH) deformation is initially and commonly observed during myopic progression, which is followed by the onset of chorioretinal atrophy.[7–9] However, most studies on the ONH and peripapillary structure have focused on glaucoma and have rarely addressed high myopia; therefore, it is important to investigate the morphological characteristics of the ONH in young myopic patients at an early stage. In addition, choroidal thinning has been found to be associated with reduced visual acuirity[10,11] and myopic chorioretinal features, including myopic macular maculopathy and myopic choroidal neovascularization, either of which may result in severe visual impairment.[12–14] Therefore, it is necessary to explore the impact of morphological characteristics of the ONH on choroidal thickness in young patients with high myopia.

Recently, Chen et al.,[15] using fundus photography, found that peripapillary atrophy (PPA) area was negatively associated with macular choroidal thickness (mChT) and peripapillary choroidal thickness (pChT), whereas tilt ratio was positively associated with mChT and negatively associated with pChT. These results indicate that myopic optic disc characteristics are associated with choroidal thinning, which is further associated with myopic chorioretinal features.[12] Optical coherence tomography (OCT) has become increasingly popular and is commonly used in clinics. Jonas et al.[16–19] and Ohno-Matsui et al.[20] considered Bruch's membrane (BM), not the sclera, to be the biomechanically supporting structure and the primary driver elongating the globe, thereby leading to choroidal thinning. Additionally, BM may have a non-negligible influence on intraocular pressure (IOP)-induced ONH deformations.[21] In this case, we speculated that BM impacts ONH deformation during the development of myopia. In addition, posterior border tissue (BT) of the sclera and BM opening at the ONH have been clearly detected on OCT images, even in patients with glaucoma accompanied by high myopia.[22,23] Compared with conventional spectral-domain OCT, swept-source OCT (SS-OCT) allows deeper penetration of tissues, especially in highly myopic eyes with axial elongation.[24]

Several studies have emphasized the importance of morphological changes in the ONH in glaucoma.[23,25] Previous studies on BT morphology focused on open-angle glaucoma. Recently, Kim et al.[26] investigated longitudinal changes in the ONH and peripapillary tissues that occur during the progression of childhood myopia; they observed that the border length (BL) increased nasally and the border tissue angle (BTA) decreased, whereas the Bruch's membrane opening distance (BMOD) remained relatively stable during the ONH and peripapillary changes. However, no study has described the associations among mChT, pChT, and morphological BT features in the ONH or peripapillary structure during the early stages of high myopia. The purpose of the present study was to investigate the morphological characteristics in the ONH and peripapillary structure (i.e., disc torsion, optic disc tilt, PPA area, vertical tilt angle, BMOD, BL, and BTA) and the associations between each of these parameters and ChT among young patients with different degrees of myopia.

Methods

Setting and Participants

This case–control study was authorized by the institutional review board and ethics committee of Shanghai General Hospital, Shanghai Jiao Tong University, and adhered to the tenets of the Declaration of Helsinki. All enrolled participants were briefed on the study protocol and signed informed consent forms.

Research Methods

The study participants were patients with high myopia attending Shanghai University in October 2016; they volunteered to participate after reading a description of the study and an open invitation to become a participant. The protocol for this cross-sectional study was consistent with those of previous studies.[15,27]

The systolic blood pressure (SBP) and diastolic blood pressure (DBP) of the students were measured. The mean arterial pressure (MAP) was calculated using the following formula: (SBP + 2 × DBP)/3. Each participant underwent a thorough ophthalmic examination, including refractive error assessment with an autorefractor instrument (KR-8900; Topcon, Tokyo, Japan), measurement of best-corrected visual acuity (BCVA) and IOP (Full Auto Tonometer TX-F; Topcon), slit-lamp biomicroscopy, color fundus examination, and measurement of the thickness of the choroid, retina, and nerve fiber layer using SS-OCT (DRI OCT-1 Atlantis; Topcon). The anterior chamber depth (ACD), central corneal thickness (CCT), lens thickness (LT), axial length (AL), and corneal radius of curvature (CR) were measured using optical low-coherence reflectometry (Aladdin; Topcon). The ratio of axial length to corneal radius (AL/CR ratio) was defined as the axial length divided by the mean corneal radius of curvature. All examinations for each patient were completed on the same day. Subjective refraction was performed by a trained optometrist. Spherical equivalent refraction (SER) was defined as the sphere plus half a cylinder. The BCVA was converted into the logarithm of minimal angle resolution (logMAR). A detailed medical history was also obtained for each participant.

Participants with high myopia were randomly selected from the 2016 Shanghai University student population. The subjects were between 16 and 28 years of age. All participants were divided into three groups based purely on the length of the ocular axis: the AL1 group had an AL $\leq$ 24 mm, the AL2 group had an AL between 26 and 27 mm, and the AL3 group had an AL $\geq$ 27 mm. The inclusion criteria were as follows: BCVA of 20/30 or better; AL $\leq$ 24 mm or $\geq$ 26 mm; SER $<$ 0.5 diopter (D); IOP $\leq$ 21 mm Hg; normal depth of the anterior chamber; and a healthy ONH without glaucomatous optic disc damage, including neuroretinal rim notching or thinning, concentric cup enlargement or shallowing, peripapillary hemorrhage, localized pallor, or peripapillary retinal nerve fiber layer thickness (pRNFLT) changes on both eyes. The exclusion criteria were as follows: (1) history of glaucoma among first-degree family members; (2) history of major systemic or ocular diseases, including congenital cataract, glaucoma, hypertension, or diabetes; (3) history of intraocular or refractive surgery; or (4) evidence of retinal pathology. In general, except for the optic disc and peripapillary changes related to myopia, the patients had no other ocular comorbidities, and only the right eye of each patient was selected for statistical analysis.

SS-OCT Imaging

The ONH, including the peripapillary and macular areas, was imaged using SS-OCT with a light source of 1050 µm

and a scanning speed of 100,000 A-scans per second, which provided a depth resolution of 8 µm and a lateral resolution of 10 µm of the tissue. The SS-OCT examinations were performed by one experienced examiner from 10:00 AM to 3:00 PM each day to minimize the influence of diurnal variation.[28,29] Using this approach, the average thicknesses of the macular retinal and choroidal layers, as well as the peripapillary retinal nerve fiber layer (RNFL) and choroidal layers, were measured. The scanning protocol used a 12-line radial scan pattern that centered on the fovea and optic disc with a resolution of 1024 × 12. Prior to scanning, the diopter values for spherical power, cylindrical power, CR, and AL were input into the SS-OCT system to minimize the magnification error, and the SS-OCT internally calculated the scan circle size based on the specific eye model from the focus settings adjusted by the device operator prior to the scan. The size of the scan diameter majorly varied with AL and partially depended on additional lens-related aspects, particularly the CR. Each layer was automatically segmented with built-in software; however, the process was inaccurate, leading to measurement artifacts, so manual segmentation was carried out.

The tomography maps were overlaid with an Early Treatment Diabetic Retinopathy Study grid (6 × 6 mm) that was focused on the macula and optic disc. The placement of the circle was manually adjusted, if necessary. Thus, each scan was divided into three concentric circles with nine regions as follows: a central circle with 1-mm diameter, an inner circle with 3-mm diameter, and an outer circle with 6-mm diameter. The inner ring (the area between the central circle and the inner circle) and the outer ring (the area between the inner circle and the outer circle) were further divided into four quadrants—namely, temporal, superior, nasal, and inferior. ChT was defined as the vertical distance between the BM and the choroidal–scleral interface. The average thickness in each sector of the grid was automatically calculated using built-in software. In the macular region, all nine sectors of the grid were applied to analyze the average thickness; however, in the parapapillary area, only four regions of the outer circle were used to calculate the average thickness because no choroidal tissue was found in the central and inner circles, and the topographic maps were not reliable in these regions.[15,28] Retinal thickness was defined as the vertical distance between the internal limiting membrane (ILM) and the interface between the photoreceptor outer segments and retinal pigment epithelium. The RNFL thickness was defined as the vertical distance between the ILM and the interface between the nerve fiber layer and the ganglion cell layer.

All measurements were conducted by a single technician experienced in analyzing OCT images. Images with a signal strength index ≤ 60 were excluded from further assessment.

Ovality Index, Torsion, and Peripapillary Atrophy Area Measurements

Color and red-free fundus photographs centered on the macula and optic disc were acquired from the same SS-OCT, which was fitted with a digital and non-mydriatic retinal camera. Two authors independently evaluated the disc photographs in random order and in a masked fashion, without any knowledge of the participants' backgrounds or diagnosis (YY and LM). The optic disc tilt, torsion, optic disc area, and vertical cup-to-disc ratio were measured using ImageJ 1.60 (National Institutes of Health, Bethesda, MD, USA). The averaged data were used for the final analysis.

Figure 1. Measurement of ovality index, torsion degree, and PPA area by ImageJ software. The dotted arrow lines indicate the longest diameter (LD) and shortest diameter (SD) of the optic disc. The ovality index was defined as the ratio between the LD and SD of the optic disc. The PPA area was outlined manually (area between the yellow dotted line and red solid line), and the pixel area was calculated automatically using the software. Torsion degree was measured between the LD and the vertical line (blue arrow line) 90° from a horizontal line (white line) connecting the fovea and the center of the optic disc.

Optic disc tilt has been referred to as the ovality index, defined as the ratio between the longest optic disc diameter and the shortest disc diameter (Fig. 1). An optic disc is classified as tilted when the ovality index ≥ 1.25.[30–33] Disc ovality has been used as a surrogate index of disc tilt.[30,34–36] The index is an objective, two-dimensional method that can be utilized on fundus photographs without the use of additional imaging devices. The results may be greatly influenced by the original shape (vertically oval) of the optic disc, so it is impossible to distinguish tilt from true disc ovality. Therefore, we used a three-dimensional measure for disc tilt—vertical tilt angle—which fully reflects the true tilt degree (described below). The optic disc margin was defined as the inner border of the peripapillary scleral ring, which was lined for measurement. The vertical meridian was defined as a vertical line perpendicular to a reference line that connected the fovea to the center of the disc. The deviation of the long axis of the optic disc from the vertical meridian was defined as the disc torsion.[9,37,38] The degree of torsion was defined as the angle between the long axis of the optic disc and the vertical meridian. Inferotemporal torsion and superonasal torsion correlated with positive and negative values of torsion, respectively. The PPA was characterized by chorioretinal atrophy adjacent to the optic disc and measured as described previously (Fig. 1).[22,23] The areas of optic disc and PPA were measured as the total number of pixels using ImageJ 1.60 software. The area was converted from pixels into square millimeters. The magnification was corrected for each AL based on Littmann's formula.[39] To assess the reproducibility of the measurements, 40 randomly selected images were re-examined by the same examiner (YY) 1 month after the initial analysis.

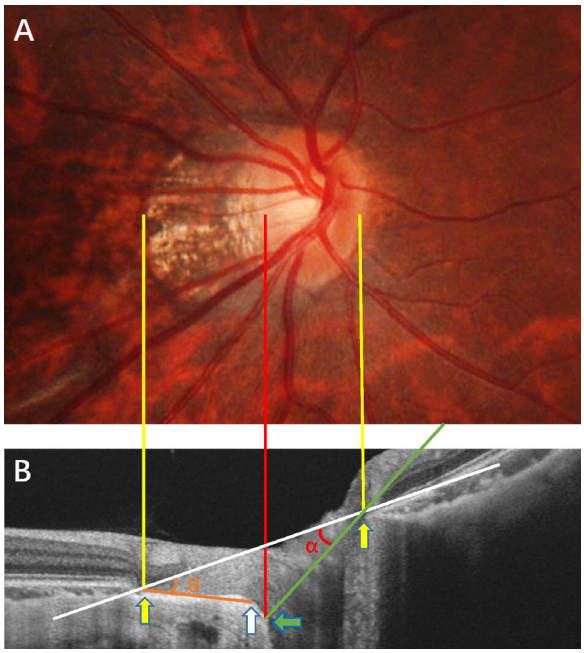

Figure 2. ONH parameter measurement in a horizontal B-scan. The nasal and temporal terminations of the BMO point (yellow arrows) and BT scleral end (white arrow) at the temporal ONH margin were identified. Optic disc boundaries were delineated on the scanning laser ophthalmoscopy images. Points at which the disc borders met BM or BT were marked on the corresponding cross-sectional OCT images. The temporal optic disc border was identified (green arrow). The line connecting the nasal and temporal BMO points was defined as the BMO reference plane (white line). The length from the temporal margin of the BMO to the border tissue scleral end was defined as the border length (orange line). The line connecting the two points, marking the clinical boundary of the disc, was defined as the ONH plane (green line). The angle between the BMO reference plane and BT at temporal location θ was defined as the BTA. The angle between the BMO reference and ONH planes at the nasal location α was defined as the vertical tilt angle.

BMOD, BL, BTA, and Vertical Tilt Angle Measurements

The vertical tilt angle, BMOD, BL, and BTA of the optic disc were measured as described previously using horizontal cross-sectional OCT images.[32,40,41] Each Bruch's membrane opening (BMO) depicted on the fundus photographs was aligned with the BMO on the respective horizontal OCT images. The BMO was defined as the innermost termination of BM. The optic disc margins were depicted on retinal images and aligned with those from horizontal cross-sectional OCT images, where they touched BM or BT (Fig. 2A). The ONH plane was defined as the line connecting two clinical disc margin points. The BMO reference plane was considered to be another line connecting both ends of the BMO. The declination between the reference plane and the ONH plane was defined as the vertical tilt angle (Fig. 2B). The BT at the temporal optic disc margin was marked on the horizontal cross-sectional OCT images. BMOD was defined as the length of the line between the two BMO points. The linear distance between the temporal BMO point and the BT/scleral end was defined and measured as the BL,[26,42] where the γ-zone PPA was located when the BT was present at the temporal optic disc margin. A built-in caliper tool within the SS-OCT was used to measure BMOD and BL. The angle between the BMO reference plane and the BT was defined as the BTA.[26] To measure the BTA and vertical tilt angle, the images were analyzed using ImageJ, and their degrees were determined using the protractor tool within ImageJ (Fig. 2B). To assess the reproducibility of the measurements, 40 randomly selected images were re-examined by the same examiner (YY) 1 month after the initial analysis.

Statistical Analysis

Statistical analysis was performed using SAS 9.4 (SAS Institute, Cary, NC, USA). The demographic and optic characteristics were reported as counts or proportions for categorical data and as means ± standard deviation for continuous data. Intra-observer (two consecutive measurements) and inter-observer (measurements by YY and LM) agreements were determined based on the intra-class correlation coefficient (ICC) using the absolute agreement model to measure the disc ovality index, torsion, PPA area, vertical tilt angle, BMOD, BL, and BTA for all participants. The distribution of all variables was examined for normality using the Kolmogorov–Smirnov test. One-way analysis of variance and the χ^2 test were used to compare the differences among the three groups, as appropriate, and the Bonferroni method was used for post hoc tests. The partial correlation analysis was used to investigate the relationship between the pChT or mChT and ocular parameters adjusted for sex. The effects of PPA area, percent with a tilted optic disc, vertical tilt angle, BMOD, BL, and BTA (independent variables) on pChT mChT, and pRNFLT (dependent variables) were assessed using multiple linear regression. The parameters that showed significant associations during the univariate analysis ($P < 0.05$) were included in the multiple linear regression analysis. The regression analysis was conducted to determine P values for the ONH-related parameters, including PPA area, BMOD, BL, BTA, and vertical tilt angle across the AL categories. After excluding the variables that showed multi-collinearity, standardized regression coefficients and adjusted coefficients of determination (R^2) were calculated from the multivariate linear regression models.

Results

General Characteristics

Among the 422 students enrolled in the study, five were excluded because of an IOP ≥ 21 mm Hg, 20 for SER ≥ 0.5 D, two for a history of refractive surgery, four for shallow anterior chamber, 12 for concentric cup enlargement, three for lost fundus examinations, and another 37 for not being of optimal quality to perform accurate measurements. Finally, the data for 339 (80.3%) students were included in the analysis. Findings for BMOD, BL, BTA, and vertical tilt angle were highly reproducible, with an ICC of 0.94 for BMOD, 0.87 for BL, 0.85 for BTA, and 0.78 for vertical tilt angle (n = 100). The thickness measurements with SS-OCT were highly reproducible in each layer, with a test–retest correlation coefficient of 0.97 to 0.99 (n = 30).

Among the 339 participants, 172 belonged to the AL1 (without high myopia) group (50.7%), 133 belonged to the AL2 group (39.2%), and 34 belonged to the AL3 group (10.0%). Both the AL2 and AL3 groups belonged to the high myopia group. The demographic and ocular characteristics of the study population are shown in Table 1. The mean

Investigative Ophthalmology & Visual Science

Table 1. Demographic and Ocular Characteristics of Study Population

Variable	Total (N = 339)	AL1 (n = 172)	AL2 (n = 133)	AL3 (n = 34)	*P*	Post Hoc
Age, y	19.83 ± 2.51	19.84 ± 2.53	19.88 ± 2.56	19.56 ± 2.25	0.80†	—
Female, n (%)	190 (56)	120 (69.8)	58 (43.6)	12 (35.3)	**<0.01**‡	AL1 > AL2/AL3
MAP, mm Hg	88.82 ± 10.85	87.28 ± 10.97	90.33 ± 10.10	90.96 ± 12.20	**0.03**†	AL1 < AL2
SER, diopter	–4.10 ± 2.73	–2.14 ± 1.59	–5.79 ± 1.95	–7.38 ± 2.32	**<0.01**†	AL1 > AL2 > AL3
BCVA, logMAR	0.02 ± 0.04	0.01 ± 0.04	0.03 ± 0.04	0.04 ± 0.05	**<0.01**†	AL1 < AL2/AL3
IOP, mm Hg	14 ± 3	14 ± 3	14 ± 3	14 ± 3	0.84†	—
ACD, mm	3.71 ± 0.26	3.60 ± 0.23	3.80 ± 0.25	3.87 ± 0.24	**<0.01**†	AL1 < AL2/AL3
CCT, µm	536 ± 36	540 ± 35	532 ± 35	531 ± 39	0.08†	—
LT, mm	3.53 ± 0.24	3.57 ± 026	3.50 ± 0.21	3.45 ± 0.18	**0.01**†	AL1 > AL2/AL3
AL, mm	25.23 ± 1.49	23.87 ± 0.50	26.39 ± 0.28	27.58 ± 0.55	**<0.01**†	AL1 < AL2 < AL3
AL/CR ratio	3.23 ± 0.17	3.12 ± 0.13	3.33 ± 0.11	3.41 ± 0.14	**<0.01**†	AL1 < AL2 < AL3
Tilted optic disc, n (%)	145 (43)	67 (39)	57 (43.5)	21 (61.8)	**0.05**‡	AL1 < AL3
Ovality index	1.23 ± 0.15	1.20 ± 0.14	1.24 ± 0.15	1.30 ± 0.16	**<0.01**†	AL1 < AL2/AL3
Torsion angle, deg	2.57 ± 17.63	3.70 ± 17.05	0.24 ± 19.11	6.23 ± 13.03	0.12†	—
PPA area, mm^2	0.51 ± 0.28	0.35 ± 0.14	0.64 ± 0.29	0.78 ± 0.29	**<0.01**†	AL1 < AL2 < AL3
BMOD, µm	2135.73 ± 531.62	1910.72 ± 419.39	2340.29 ± 545.87	2473.84 ± 490.94	**<0.01**†	AL1 < AL2/AL3
BL, µm	507.01 ± 293.61	376.27 ± 263.41	627.58 ± 247.21	696.75 ± 306.92	**<0.01**†	AL1 < AL2/AL3
BTA, deg	82.47 ± 45.15	96.31 ± 50.97	68.23 ± 33.77	68.19 ± 28.72	**<0.01**†	AL1 > AL2/AL3
Vertical tilt angle, deg	11.34 ± 6.89	9.20 ± 7.20	13.15 ± 5.63	15.04 ± 6.32	**<0.01**†	AL1 < AL2 < AL3
pChT, µm	137.63 ± 42.00	151.52 ± 42.66	124.34 ± 35.30	111.93 ± 32.83	**<0.01**†	AL1 > AL2/AL3
pRNFLT, µm	102.37 ± 8.84	101.73 ± 8.44	102.58 ± 9.36	104.90 ± 8.90	0.23†	—
mChT, µm	221.99 ± 62.47	248.61 ± 59.55	199.65 ± 54.49	178.26 ± 46.34	**<0.01**†	AL1 > AL2/AL3
mRT, µm	277.34 ± 12.80	280.18 ± 12.82	274.85 ± 12.95	273.09 ± 8.52	**<0.01**†	AL1 > AL2/AL3

Factors with statistical significance are shown in bold.
*Multiple comparisons among the three axial length groups.
† One-way ANOVA test.
‡ χ^2 test.

ages of the AL1, AL2, and AL3 groups were 19.84 ± 2.53 years, 19.88 ± 2.56 years, and 19.56 ± 2.25 years, respectively. The mean SER error was –2.14 ± 1.59 D in the AL1 group, –5.79 ± 1.95 D in the AL2 group, and –7.38 ± 2.32 D in the AL3 group. No significant differences in age, IOP, CCT, or torsion angle were observed in the various myopia groups ($P > 0.05$). However, the number of female patients with high myopia was higher than the number of those without high myopia ($P < 0.01$). Patients with high myopia had a significantly higher MAP ($P < 0.01$), worse BCVA ($P < 0.01$), deeper ACD ($P < 0.01$), thinner LT ($P < 0.01$), higher AL/CR ratio ($P < 0.01$), and larger ovality index ($P < 0.01$) compared with those without high myopia.

Changes in the Structural Parameters Using SS-OCT

As shown in Table 1, significant differences were found in various structural parameters in the macular and optic disc areas in different myopic groups using SS-OCT. pChT, mChT, and macular retinal thickness (mRT) (all, $P < 0.01$) were significantly thinner in patients with high myopia than in those without high myopia. Furthermore, the AL3 group had a significantly larger PPA area and vertical tilt angle compared with the AL1 and AL2 groups. BMOD and BL were longer and the BTA was smaller in patients with high myopia compared with patients without high myopia. No significant differences in the pRNFLT were observed among the groups.

Correlations Between mChT and the Morphological Characteristics of the ONH and Peripapillary Structure

Partial correlation coefficients between mChT and ocular parameters after adjusting for sex are summarized in Table 2. mChT was negatively associated with BMOD ($r = –0.51$, $P < 0.01$), followed by AL ($r = –0.49$, $P < 0.01$), PPA area ($r = –0.44$, $P < 0.01$), BL ($r = –0.39$, $P < 0.01$), ovality index ($r = –0.26$, $P < 0.01$), vertical tilt angle ($r = –0.24$, $P < 0.01$), and BCVA ($r = –0.12$, $P = 0.05$); mChT was positively associated with BTA ($r = 0.48$, $P < 0.01$) and SER ($r = 0.41$, $P < 0.01$).

Table 2. Partial Correlation Analysis Between Choroidal Thickness and Ocular Parameters Adjusted for Sex

	Macular Choroidal Thickness, µm		Peripapillary Choroidal Thickness, µm	
Variable	*r*	*P*	*r*	*P*
BMOD, µm	–0.51	<0.01	–0.29	<0.01
BL, µm	–0.39	<0.01	–0.23	<0.01
BTA, deg	0.48	<0.01	0.31	<0.01
Vertical tilt angle, deg	–0.24	<0.01	–0.15	0.02
PPA area, mm^2	–0.44	<0.01	–0.34	<0.01
Presence of tilted optic disc	–0.07	0.30	–0.05	0.40
Ovality index	–0.26	<0.01	–0.15	0.03
AL, mm	–0.49	<0.01	–0.44	<0.01
SER, diopter	0.41	<0.01	0.34	<0.01
BCVA, logMAR	–0.12	0.05	–0.15	0.02
Age, y	0.00	0.96	0.04	0.51
MAP, mm Hg	0.28	0.18	0.07	0.29
IOP, mm Hg	0.03	0.69	0.06	0.33
ACD, mm	–0.04	0.56	–0.06	0.35
CCT, µm	0.10	0.12	0.06	0.31
LT, mm	0.07	0.25	0.12	0.06

Multivariate regression analysis adjusted for age and sex was used to identify independent factors associated with mChT. Because the current study focused on the morphological characteristics of the ONH and ChT in axial myopia and because the explanatory power of the AL and percentage of eyes with a tilted optic disc for the change was greater

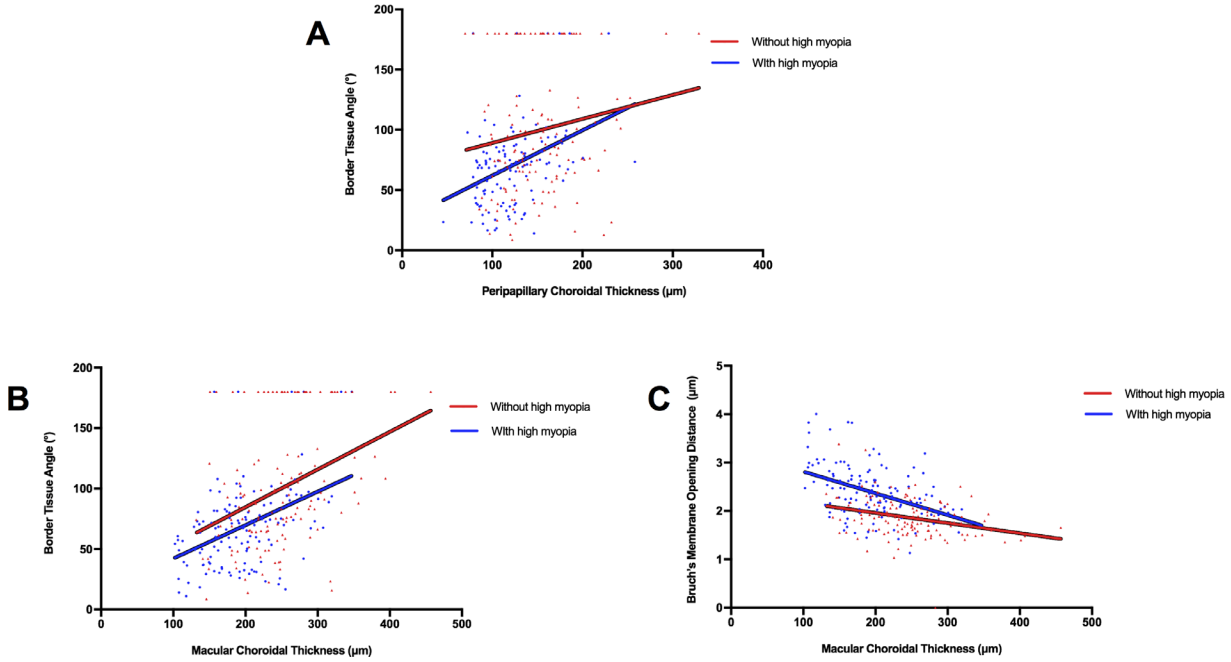

Figure 3. (**A**) Linear correlation between the average pChT and BTA in groups with and without high myopia. (**B**) Linear correlation between the average mChT and BTA in groups with and without high myopia. (**C**) Linear correlation between the average mChT and BMOD in groups with and without high myopia.

Table 3. Multivariate Regression Analysis of Associations with Macular Choroidal Thickness in All Subjects

Variable	*B*	*β*	*P*
Sex (male:female)	–8.54	–0.07	0.21
Age, y	–1.42	–0.06	0.26
AL, mm	–9.72	–0.23	**<0.01**
Presence of tilted optic disc	12.21	0.09	0.09
PPA area, mm^2	–28.43	–0.13	0.07
BMOD, µm	–35.80	–0.31	**<0.01**
BL, µm	38.22	0.18	0.06
BTA, deg	0.32	0.23	**<0.01**
Vertical tilt angle, deg	–1.28	–0.14	0.10

Adjusted for all variables listed. R^2 for all subjects = 0.367. Factors with statistical significance are shown in bold.

Table 4. Multivariate Regression Analysis of Associations with Peripapillary Choroidal Thickness in All Subjects

Variable	*B*	*β*	*P*
Sex (male:female)	–15.95	–0.19	**<0.01**
Age, y	0.01	0.00	0.99
AL, mm	–11.98	–0.43	**<0.01**
Presence of tilted optic disc	7.93	0.09	0.16
PPA area, mm^2	–15.99	–0.11	0.18
BMOD, µm	0.15	0.00	0.98
BL, µm	31.04	0.22	0.06
BTA, deg	0.26	0.29	**<0.01**
Vertical tilt angle, deg	–0.17	–0.03	0.76

Adjusted for all variables listed. R^2 for all subjects = 0.247. Factors with statistical significance are shown in bold.

than that of the spherical equivalent and ovality index, only variations in AL and percentage of eyes with tilted optic disc were used for multivariate regression analysis. The analysis revealed that AL, BMOD, and BTA were independently associated with mChT (all, $P < 0.01$). According to the model, every 1-mm increase in AL was associated with a 9.72-µm decrease in mChT; every 1-µm increase in BMOD was associated with a 35.80-µm decrease in mChT (Fig. 3C); and every 1° increase in BTA was associated with a 0.32-µm increase in mChT (Fig. 3B). The combination of these factors yielded an adjusted R^2 of 0.367 (Table 3).

Correlations Between pChT and the Morphological Characteristics of the ONH and Peripapillary Structure

Partial correlation coefficients between pChT and ocular parameters after adjusting for sex are summarized in Table 2. Similar to mChT, pChT was negatively associated with AL ($r = –0.44$, $P < 0.01$), followed by PPA area ($r = –0.34$, $P < 0.01$), BMOD ($r = –0.29$, $P < 0.01$), BL ($r = –0.23$, $P < 0.01$), vertical tilt angle ($r = –0.15$, $P = 0.02$), BCVA ($r = –0.15$, $P = 0.02$), and ovality index ($r = –0.15$, $P = 0.03$); pChT was positively associated with SER ($r = 0.34$, $P < 0.01$) and BTA ($r = 0.31$, $P < 0.01$).

Multivariate regression analysis adjusted for age and sex was used to identify independent factors associated with pChT. The analysis revealed that sex, AL, and BTA were independently associated with pChT (all, $P < 0.01$). According to the model, every 1-mm increase in AL was associated with a 11.98-µm decrease in pChT, and every 1° increase in BTA was associated with a 0.26-µm increase in pChT (Fig. 3A). The combination of these factors yielded an adjusted R^2 of 0.247 (Table 4).

Correlations Among BMOD, BL, BTA, Vertical Tilt Angle, PPA Area, and AL

The associations among BMOD, BL, BTA, vertical tilt angle, PPA area, and AL were further investigated separately. Linear

Table 5. Multivariate Regression Analysis of Associations with Peripapillary Retinal Nerve Fiber Layer Thickness in All Subjects

Variable	*B*	β	*P*
Sex (male:female)	0.32	0.18	**0.01**
Age, y	0.07	0.02	0.75
IOP, mm Hg	–0.24	0.08	0.25
AL, mm	0.26	0.05	0.62
Presence of tilted optic disc	–0.27	–0.02	0.84
PPA area, mm^2	3.83	0.13	0.17
BMOD, µm	3.71	0.23	**0.03**
BL, µm	–9.03	–0.31	**0.02**
BTA, deg	0.01	0.03	0.75
Vertical tilt angle, deg	0.27	0.22	0.05

Adjusted for all variables listed. R^2 for all subjects = 0.039. Factors with statistical significance are shown in bold.

regression analysis showed that AL was positively associated with PPA area ($\beta = 0.60$, $P < 0.01$), BMOD ($\beta = 0.49$, $P < 0.01$), BL ($\beta = 0.47$, $P < 0.01$), and vertical tilt angle ($\beta = 0.35$, $P < 0.01$) and was negatively associated with BTA ($\beta = –0.36$, $P < 0.01$).

Discussion

This cross-sectional study found that individuals with longer AL presented with a longer BMOD and BL, larger PPA area and vertical tilt angle, and smaller BTA; also, AL was correlated with enlargement of the globe with axial myopia. After adjusting for other parameters, including PPA area, BMOD was found to be negatively associated with mChT, and BTA was found to be positively correlated with mChT and pChT; no associations were found between PPA area and ChT. According to the clinical observations, ChT in high myopia may continue to reduce with age and lead to more severe myopic chorioretinopathy. The popularity of OCT in clinical practice suggests that we should pay more attention to BT configurations in young patients with myopia on OCT scans at an early stage to identify early-risk populations with fundus lesions.

Our main purpose was to investigate morphological characteristics of the ONH and peripapillary structure and the associations between ChT and these parameters, which are more associated with myopic shift and visual acuity during early myopic progression in young healthy highly myopic eyes. However, the current work was also partially motivated by a need to explore the relationship between glaucoma and ONH characteristics in myopia. The impact of the morphological characteristics of the ONH on pRNFLT, of which abnormal patterns are considered to be diagnostic markers for the glaucoma,[43] cannot be ignored. In the current study, no significant differences in the pRNFLT were observed among the different AL groups (Table 1). Our findings are consistent with those of previous studies.[44–46] Even so, multivariate regression analysis adjusted for age and sex was carried out to identify independent factors associated with pRNFLT. The combination of these factors yielded an adjusted R^2 of 0.039 (Table 5), indicating that these myopia-related ONH parameters could not explain the variance of pRNFLT in the current study.

This study was novel in investigating the correlations between ChT and early morphological characteristics of the ONH and peripapillary structure, based on SS-OCT of patients with high myopia. It demonstrated negative correlations between mChT and BMOD and positive correlations among mChT, pChT, and BTA. Previous studies have shown a significant association between PPA area and high myopia.[8,23] A recent study by our team suggested that PPA area in young patients with high myopia correlated significantly and negatively with pChT and mChT, even in early myopic stages.[15] The present study found that BMOD and BTA were more sensitive independent factors associated with mChT compared with PPA area (Table 3), and BTA could be a more sensitive independent factor associated with pChT (Table 4).

The reason why the correlations among BMOD, BTA, and mChT were greater than that between PPA area and mChT might be that BMOD is a comprehensive variable, responding to the severity of the BM defect and deformation of the eyeball based on three dimensions, whereas PPA area might have responded only to the severity of the BM defect. Another reason could be that PPA measurements were based solely on fundus photography and influenced the results subjectively to some extent; however, BMOD and BTA measurements were based on SS-OCT, so the results were relatively more objective and accurate. It was also speculated that an increase in BMOD and a decrease in BTA preceded enlargement of the PPA area with the progression of myopia and the accompanying deformation of the eyeball. Compared with PPA area, BMOD and BTA were earlier indicators for predicting fundus lesions in high myopia. Given that OCT has been widely used in clinical practice, it is necessary to use OCT to assess morphological characteristics of the optic disc and peripapillary structure, especially the BT features, in early screening and to screen out high-risk groups as much as possible.

Few studies have investigated the ultrastructural changes (i.e., morphological features of BT at the temporal disc margin and measurement of BMOD, BL, and BTA on horizontal cross-sectional OCT scans) related to BM in high myopia. A significantly positive correlation was identified between AL and BMOD in the present study, a finding that differs from the results of a previous study.[26] The reasons for the discrepancy in BMOD between these studies could perhaps be explained as follows. First, the sample sizes were different. Only 23 patients were enrolled in the study by Kim et al.,[26] whereas the present study included 339 individuals with different refractive statuses, including 167 patients with high myopia. Second, characteristics of the participants, such as ethnicity and age, differed. The participants enrolled in the study by Kim et al.[26] were children ages 6.7 to 12.5 years at the baseline, and the prospective longitudinal study spanned 2 years. The structure of the optic disc in children compared with adults might be more stable with the progression of myopia, suggesting that BMODs might not have changed during the study period. It was hypothesized that physiological growth could partly counteract the effects of rapid axial elongation during the progression of myopia in children until the axial elongation became the determining factor of BMOD. This hypothesis stemmed from consistent findings of previous studies on choroidal thinning in children between the ages of 6 and 19 years.[47]

In addition, Lee et al.[42] and Kim et al.[26] both reported that deep structures of the ONH, including the lamina cribrosa and temporal BT, moved somewhat nasally during myopic progression in children, resulting in temporal BM defects. Based on the results of the present study and previous stud-

Investigative Ophthalmology & Visual Science

ies, it could be concluded that, due to a physiological protective effect, BMOD remained stable but the BT had already shifted nasally from BMO. However, with further elongation of the globe, the drawing back of both ends of BM was involved in the BM defect. As a consequence, BMOD and BL became longer, and the BTA became smaller. Therefore, close monitoring of BMOD, BL, and BTA is essential for young adults with high myopia, even at an early stage. Further prospective studies are needed to better understand the structural changes in the ONH and peripapillary structure.

This study had several limitations. First, the scanning line of the OCT images did not align with the fovea-to-disc lines, which might have resulted in measurement errors for BMOD, BL, BTA, and vertical tilt angle. Second, the sample size was relatively small, and the cases were rather limited in terms of age. Still, the present study showed significant morphological changes in the ONH among the groups, and further studies on patients of various ages with high myopia should be conducted. Third, the OCT image was exported at a ratio of 1:1, which might be inaccurate with the actual eyeball shape; however, this did not affect observing a trend in BT configuration and vertical tilt angle changes. Given that the visual field defects in the patients were not assessed, not all patients with glaucoma might have been removed. Because the students in the present study were of a younger age, the likelihood of confounding diseases, such as glaucoma and cataract, influencing the findings was negligible. Finally, this study was a cross-sectional study; hence, causal relationships between the morphologic characteristics of the optic disc and ChT were not determined.

In conclusion, this study is novel in reporting that longer BMOD positively correlated with lower mChT, and a smaller BTA correlated positively with lower mChT and pChT in young adults, especially in patients with high myopia; however, no correlation was found between PPA area and ChT in the same multiple regression model. Thus, morphological characteristics of BT, such as BMOD, BL, and BTA, could serve as early indicators of high myopia progressing to pathological myopia. The findings indicate that it is essential to combine fundus photographs with OCT scans to assess morphological characteristics of the ONH and peripapillary structure in the early screening of high myopia so as to identify more high-risk cases.

Acknowledgments

Supported by grants from the National Natural Science Foundation of China (81703287), the National Key R&D Program of China (2016YFC0904800, 2019YFC0840607), the Shanghai Science and Technology Commission Research Project (17ZR1426900), and the National Science and Technology Major Project of China (2017ZX09304010). The funding organizations had no role in the design, conduct, analysis, or publication of this study.

Disclosure: **G. Hu**, None; **Q. Chen**, None; **X. Xu**, None; **H. Lv**, None; **Y. Du**, None; **L. Wang**, None; **Y. Yin**, None; **Y. Fan**, None; **H. Zou**, None; **J. He**, None; **J. Zhu**, None; **X. Xu**, None

References

1. Morgan IG, Ohno-Matsui K, Saw S-M. Myopia. *Lancet*. 2012;379:1739–1748.
2. Ohno-Matsui K, Akiba M, Moriyama M, et al. Acquired optic nerve and peripapillary pits in pathologic myopia. *Ophthalmology*. 2012;119:1685–1692.
3. Xu L, Wang Y, Li Y, et al. Causes of blindness and visual impairment in urban and rural areas in Beijing: the Beijing Eye Study. *Ophthalmology*. 2006;113:1134.e1–e11.
4. Mitchell P, Hourihan F, Sandbach J, Wang JJ. The relationship between glaucoma and myopia: the Blue Mountains Eye Study. *Ophthalmology*. 1999;106:2010–2015.
5. Grodum K, Heijl A, Bengtsson B. Refractive error and glaucoma. *Acta Ophthalmol Scand*. 2001;79:560–566.
6. Shen L, Melles RB, Metlapally R, et al. The association of refractive error with glaucoma in a multiethnic population. *Ophthalmology*. 2016;123:92–101.
7. Nakazawa M, Kurotaki J, Ruike H. Longterm findings in peripapillary crescent formation in eyes with mild or moderate myopia. *Acta Ophthalmol*. 2008;86:626–629.
8. Kim TW, Kim M, Weinreb RN, Woo SJ, Park KH, Hwang JM. Optic disc change with incipient myopia of childhood. *Ophthalmology*. 2012;119:21–26.e1–e3.
9. Samarawickrama C, Mitchell P, Tong L, et al. Myopia-related optic disc and retinal changes in adolescent children from Singapore. *Ophthalmology*. 2011;118:2050–2057.
10. Flores-Moreno I, Ruiz-Medrano J, Duker JS, Ruiz-Moreno JM. The relationship between retinal and choroidal thickness and visual acuity in highly myopic eyes. *Br J Ophthalmol*. 2013;97:1010–1013.
11. Nishida Y, Fujiwara T, Imamura Y, Lima LH, Kurosaka D, Spaide RF. Choroidal thickness and visual acuity in highly myopic eyes. *Retina*. 2012;32:1229–1236.
12. Neelam K, Cheung CMG, Ohno-Matsui K, Lai TYY, Wong TY. Choroidal neovascularization in pathological myopia. *Prog Retin Eye Res*. 2012;31:495–525.
13. Ohno-Matsui K, Kawasaki R, Jonas JB, et al. International photographic classification and grading system for myopic maculopathy. *Am J Ophthalmol*. 2015;159:877–883.e7.
14. Koh V, Tan C, Tan PT, et al. Myopic maculopathy and optic disc changes in highly myopic young Asian eyes and impact on visual acuity. *Am J Ophthalmol*. 2016;164:69–79.
15. Chen Q, He J, Yin Y, et al. Impact of the morphologic characteristics of optic disc on choroidal thickness in young myopic patients. *Invest Opthalmol Vis Sci*. 2019;60:2958–2967.
16. Jonas JB, Xu L. Histological changes of high axial myopia. *Eye (Lond)*. 2014;28:113–117.
17. Jonas JB, Panda-Jonas S. Secondary Bruch's membrane defects and scleral staphyloma in toxoplasmosis. *Acta Ophthalmol*. 2016;94:e664–e666.
18. Jonas JB, Ohno-Matsui K, Jiang WJ, Panda-Jonas S. Bruch membrane and the mechanism of myopization: a new theory. *Retina*. 2017;37:1428–1440.
19. Jonas JB, Panda-Jonas S. [Epidemiology and anatomy of myopia]. *Ophthalmologe*. 2019;116:499–508.
20. Ohno-Matsui K, Jonas JB. Posterior staphyloma in pathologic myopia. *Prog Retin Eye Res*. 2019;70:99–109.
21. Wang X, Teoh CKG, Chan ASY, Thangarajoo S, Jonas JB, Girard MJA. Biomechanical properties of Bruch's membrane-choroid complex and their influence on optic nerve head biomechanics. *Invest Opthalmol Vis Sci*. 2018;59:2808–2817.
22. Dai Y, Jonas JB, Huang H, Wang M, Sun X. Microstructure of parapapillary atrophy: beta zone and gamma zone. *Invest Ophthalmol Vis Sci*. 2013;54:2013–2018.
23. Vianna JR, Malik R, Danthurebandara VM, et al. Beta and gamma peripapillary atrophy in myopic eyes with and without glaucoma. *Invest Ophthalmol Vis Sci*. 2016;57:3103.

24. Potsaid B, Baumann B, Huang D, et al. Ultrahigh speed 1050nm swept source/Fourier domain OCT retinal and anterior segment imaging at 100,000 to 400,000 axial scans per second. *Opt Express*. 2010;18:20029–20048.
25. Jonas JB, Wang YX, Zhang Q, et al. Parapapillary gamma zone and axial elongation-associated optic disc rotation: the Beijing Eye Study. *Invest Ophthalmol Vis Sci*. 2016;57:396–402.
26. Kim M, Choung HK, Lee KM, Oh S, Kim SH. Longitudinal changes of optic nerve head and peripapillary structure during childhood myopia progression on OCT: Boramae Myopia Cohort Study report 1. *Ophthalmology*. 2018;125:1215–1223.
27. He J, Chen Q, Yin Y, et al. Association between retinal microvasculature and optic disc alterations in high myopia. *Eye (Lond)*. 2019;33:1494–1503.
28. Deng J, Li X, Jin J, et al. Distribution pattern of choroidal thickness at the posterior pole in Chinese children with myopia. *Invest Ophthalmol Vis Sci*. 2018;59:1577–1586.
29. Tan CS, Ouyang Y, Ruiz H, Sadda SR. Diurnal variation of choroidal thickness in normal, healthy subjects measured by spectral domain optical coherence tomography. *Invest Ophthalmol Vis Sci*. 2012;53:261–266.
30. Tay E, Seah SK, Chan S-P, et al. Optic disk ovality as an index of tilt and its relationship to myopia and perimetry. *Am J Ophthalmol*. 2005;139:247–252.
31. Vongphanit J, Mitchell P, Wang JJ. Population prevalence of tilted optic disks and the relationship of this sign to refractive error. *Am J Ophthalmol*. 2002;133:679–685.
32. Hosseini H, Nassiri N, Azarbod P, et al. Measurement of the optic disc vertical tilt angle with spectral-domain optical coherence tomography and influencing factors. *Am J Ophthalmol*. 2013;156:737–744.
33. Takasaki H, Higashide T, Takeda H, Ohkubo S, Sugiyama K. Relationship between optic disc ovality and horizontal disc tilt in normal young subjects. *Jpn J Ophthalmol*. 2013;57:34–40.
34. Jonas JB, Kling F, Grundler AE. Optic disc shape, corneal astigmatism, and amblyopia. *Ophthalmology*. 1997;104:1934–1937.
35. Giuffre G. Chorioretinal degenerative changes in the tilted disc syndrome. *Int Ophthalmol*. 1991;15:1–7.
36. How AC, Tan GS, Chan YH, et al. Population prevalence of tilted and torted optic discs among an adult Chinese population in Singapore: the Tanjong Pagar Study. *Arch Ophthalmol*. 2009;127:894–899.
37. Park HY, Lee K, Park CK. Optic disc torsion direction predicts the location of glaucomatous damage in normal-tension glaucoma patients with myopia. *Ophthalmology*. 2012;119:1844–1851.
38. Lee KS, Lee JR, Kook MS. Optic disc torsion presenting as unilateral glaucomatous-appearing visual field defect in young myopic Korean eyes. *Ophthalmology*. 2014;121:1013–1019.
39. Bennett AG, Rudnicka AR, Edgar DF. Improvements on Littmann's method of determining the size of retinal features by fundus photography. *Graefes Arch Clin Exp Ophthalmol*. 1994;232:361–367.
40. Park HY, Choi SI, Choi JA, Park CK. Disc torsion and vertical disc tilt are related to subfoveal scleral thickness in open-angle glaucoma patients with myopia. *Invest Opthalmol Vis Sci*. 2015;56:4927–4935.
41. Sung MS, Lee TH, Heo H, Park SW. Association between optic nerve head deformation and retinal microvasculature in high myopia. *Am J Ophthalmol*. 2018;188:81–90.
42. Lee KM, Choung HK, Kim M, Oh S, Kim SH. Positional change of optic nerve head vasculature during axial elongation as evidence of lamina cribrosa shifting. *Ophthalmology*. 2018;125:1224–1233.
43. Quigley HA. Glaucoma. *Lancet*. 2011;377:1367–1377.
44. Savini G, Barboni P, Parisi V, Carbonelli M. The influence of axial length on retinal nerve fibre layer thickness and optic-disc size measurements by spectral-domain OCT. *Br J Ophthalmol*. 2012;96:57–61.
45. Kang SH, Hong SW, Im SK, Lee SH, Ahn MD. Effect of myopia on the thickness of the retinal nerve fiber layer measured by Cirrus HD optical coherence tomography. *Invest Ophthalmol Vis Sci*. 2010;51:4075–4083.
46. Wang M, Elze T, Li D, et al. Age, ocular magnification, and circumpapillary retinal nerve fiber layer thickness. *J Biomed Opt*. 2017;22:1–19.
47. Xiong S, He X, Deng J, et al. Choroidal thickness in 3001 Chinese children aged 6 to 19 years using swept-source OCT. *Sci Rep*. 2017;7:45059.